Article

Pharmacokinetics and tumour disposition of PEGylated, methotrexate conjugated poly-L-lysine dendrimers

lisa m kaminskas, brian kelly, victoria m McLeod, Ben J Boyd, guy krippner, Elizabeth D Williams, and Christopher John Porter

Mol. Pharmaceutics, **Just Accepted Manuscript** • Publication Date (Web): 19 May 2009

Pharmacokinetics and tumour disposition of PEGylated, methotrexate conjugated poly-L-lysine dendrimers

Lisa M Kaminskas[1], Brian D Kelly[2], Victoria M McLeod[1], Ben J Boyd[1], Guy Y Krippner[2], Elizabeth D Williams[3], Christopher JH Porter[1]

[1] Drug Delivery, Disposition and Dynamics, Monash Institute of Pharmaceutical Sciences, Monash University (Parkville campus), 381 Royal Pde, Parkville, VIC, 3052, AUSTRALIA.

[2] Starpharma Pty. Ltd., Level 6, Baker Heart Research Building, Commercial Rd, Melbourne, VIC, 3004, AUSTRALIA

3 Centre for Cancer Research, Monash Institute of Medical Research, Monash University, 246 Clayton Rd, Clayton, VIC, 3168, AUSTRALIA.

*Corresponding author: chris.porter@pharm.monash.edu.au

TITLE RUNNING HEAD: Pharmacokinetics of methotrexate/PEG-poly-L-lysine dendrimers

CORRESPONDING AUTHOR FOOTNOTE: Christopher JH Porter. Phone: +61399039649; Fax: +61399039583.

TOC

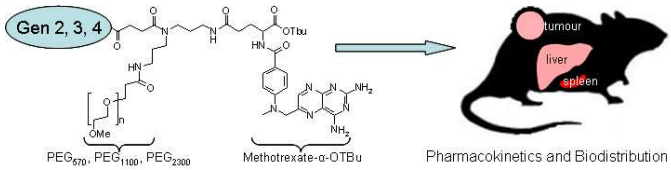
Gen 2, 3, 4
OTbu
OMe
n
PEG570, PEG1100, PEG2300
Methotrexate-α-OTBu
tumour
liver
spleen
Pharmacokinetics and Biodistribution

Abstract:

Dendrimers have potential for delivering chemotherapeutic drugs to solid tumours via the enhanced permeation and retention (EPR) effect. The impact of conjugation of hydrophobic anticancer drugs to hydrophilic PEGylated dendrimer surfaces, however, has not been fully investigated. The current study has therefore characterised the effect on dendrimer disposition of conjugating α-carboxyl protected methotrexate (MTX) to a series of PEGylated ^{3}H-labelled poly-L-lysine dendrimers ranging in size from generation 3 (G3) to 5 (G5) in rats. Dendrimers contained 50% surface PEG and 50% surface MTX. Conjugation of MTX generally increased plasma clearance when compared to conjugation with PEG alone. Conversely, increasing generation reduced clearance, increased metabolic stability and reduced renal elimination of the administered radiolabel. For constructs with molecular weights >20 kDa increasing the molecular weight of conjugated PEG also reduced clearance and enhanced metabolic stability but had only a minimal effect on renal elimination. Tissue distribution studies revealed retention of MTX conjugated smaller (G3-G4) PEG_{570} dendrimers (or their metabolic products) in the kidneys. In contrast, the larger G5 dendrimer was concentrated more in the liver and spleen. The G5 PEG_{1100} dendrimer was also shown to accumulate in solid Walker 256 and HT1080 tumours and comparative disposition data in both rats (1 to 2% dose/g in tumour) and mice (11% dose/g in tumour) are presented. The results of this study further illustrate the potential utility of biodegradable PEGylated poly-L-lysine dendrimers as long-circulating vectors for the delivery and tumour-targeting of hydrophobic drugs.

Introduction:

Several approaches have been explored in an attempt to achieve site specific chemotherapy, including localised drug administration[1], antibody mediated targeting[2], and exploitation of abnormalities in the vascular structure and lymphatic drainage of solid tumours via the enhanced permeation and retention (EPR) effect[3]. Tumour targeting via the EPR effect has received considerable attention[3] and a large range of nanoparticular carriers (liposomes, polymeric micelles, nanoparticles) and macromolecules (proteins, polymers, dendrimers) have been evaluated for their potential to enhance the biodistribution of chemotherapeutics to solid tumours[3-6].

A number of commonalities are evident in delivery systems that achieve effective EPR in tumour tissue. These include a requirement for molecular size (or particle size in the case of a colloidal carrier) to be larger than the threshold for renal filtration and the presentation of a hydrophilic interaction surface to the biological environment to reduce enzymatic cleavage or phagocytic abstraction[3, 4, 7]. In turn, these properties provide for extended circulation times after intravenous administration and the opportunity for enhanced extravasation at sites of enhanced vascular permeability (such as that within many solid tumours). Stealth liposomes with hydrodynamic diameters of 100-200 nm have been shown to provide some degree of tumour targeting and to release encapsulated drug over extended periods of time[4]. Indeed doxorubicin encapsulated in a PEGylated liposome (Doxil®) is currently used to treat a range of solid tumours including breast and ovarian carcinomas, prostate cancer and Karposi's sarcoma[8]. A number of reports have also described improved chemotherapy and decreased systemic toxicity via the conjugation of anticancer drugs, including doxorubicin or methotrexate (MTX), to

polymers[9-16]. Several PEGylated dendronised polymers have also been examined as drug delivery systems that may improve the circulation time, tumour targeting, anti-tumour efficacy and systemic toxicity of surface conjugated drugs.[12, 17-21] In each of these cases, surface PEGylation was used to reduce accumulation of the dendrimers into reticuloendothelial organs and increase plasma circulation times such that tumour targeting via EPR could be enhanced. The influence of PEG load and size on the plasma residence of dendrimers has previously been characterised[18, 22], however, the impact of drug conjugation on the stealth effects imparted by PEGylation has not been evaluated. This is potentially significant since many anticancer drugs are hydrophobic and as such their presence is likely to change the surface characteristics and in vivo behaviour of the PEGylated dendrimer carriers.

In the current study therefore, G2 to G4 poly-lysine dendrimers were capped with succinimyldipropyldiamine ($SuN(PN)_2$, abbreviated to SPN in subsequent dendrimer nomanclature) derived wedges comprising 50% PEG (570-2300 Da) and 50% methotrexate to form G3 to G5 PEGylated, MTX-linked dendrimers and their intravenous pharmacokinetics, plasma stability and tissue deposition profiles examined. The symmetrical analogue of lysine was employed in an attempt to potentially enhance metabolic stability (and therefore circulation time) since previous studies have shown a marked increase in metabolic stability for L-lysine dendrimer cores when capped with a non-natural layer such as D-lysine[23]. In these studies, methotrexate was linked via a stable amide linker since use of a cleavable linkage would preclude accurate investigation of the effects of drug conjugation on the pharmacokinetic properties of the intact dendrimer due to liberation of drug and exposure of the linker and dendrimer scaffold by enzymatic degradation. The largest G5 dendrimer (containing a 50% PEG_{1100} surface) was also examined for potential

tumour accumulation via the EPR effect and a comparative study of tumour uptake in rats and mice conducted. In addition, since the dendrimers employed in the current study were prepared using a symmetrical analogue of lysine in the final lysine generation (succinimyldipropyldiamine, Figure 1) the pharmacokinetics and disposition have been compared to the equivalent *all*-L-lysine (ie. natural lysine) fully PEGylated dendrimers described previously.

Methods:

Materials

Buffer reagents were purchased from Aldrich and were used without further purification. N-(benzyloxycarbonyl)-3-bromopropylamine and mono-BOC-1,3-diamino propane were purchased from High Force Research Ltd (Durham, England). Unlabelled lysine for synthesis was purchased from Bachem (Bunbendorf, Switzerland). Soluene-350 and Starscint were purchased from Packard Biosciences (Meriden, CT). Heparin (10,000 U/ml) was obtained from Faulding (SA, Australia). Saline was from Baxter Healthcare (NSW, Australia). Medium 199, Minimum Essential Medium (MEM) with Earles salts, trypsin-EDTA (0.25%) and non-essential amino acids (NEAA) were purchased from Sigma (NSW, Australia). Hanks Balanced Salt Solution (HBSS), foetal bovine serum (FBS), horse serum, Glutamax and penicillin-streptomycin were from Gibco (NY, USA). Cell culture flasks (75 cm^2) were from Corning (NY, USA). Isopropyl alcohol was AR grade and was purchased from Mallinckrodt Chemicals (Phillipsburg, USA). All other solvents were HPLC grade and were used without any further purification. (L)-(4,5-^{3}H)-lysine (1 mCi/ml)

was purchased from MP Biomedicals (Irvine, CA, USA). Monodisperse $PEG_{570}NHS$, $PEG_{1100}NHS$ and $PEG_{2300}NHS$ were purchased from Quanta BioDesign, Ltd (USA).

Synthesis of radiolabelled dendrimers.

The tritium radiolabel was incorporated using a lysine moiety that contained tritium labels at the γ and δ positions and in all cases the tritium labelled lysine was used in the outermost lysine layer of the dendrimer scaffold. A similar nomenclature for the dendrimers has been described previously[23], but briefly, dendrimers generated using an outer generation of $SuN(PN)_2$ are represented as $GX(SPN)\text{-}(PEG_Y)_Z(drug)_Z$ or $GX(SPN)\text{-}(PEG_Y)_Z$, where X represents the final dendrimer generation (including the outer SPN layer), SPN is abbreviated notation for $SuN(PN)_2$ and refers to an outer layer composed of succinimyldipropyldiamine (a symmetrical analogue of lysine), Y represents the MW of the PEG chain and Z represents the number of PEG and drug molecules attached to the surface. Fully PEGylated dendrimers containing all L-lysine scaffolding which were previously referred to as $Lys_X(PEG_Y)_{2X}$, where X is the number of lysines in the outer generation and Y is the PEG MW[22], have in the current paper been referred to as $GX(Lys)\text{-}(PEG_Y)_Z$, in order to be consistent with the notation used for dendrimers composed with an outer generation of $SuN(PN)_2$. In these studies, methotrexate (MTX) was chosen as a model hydrophobic anticancer drug. For the purposes of this study the free carboxylic acid group of MTX was *tert*-butyl protected in an attempt to prevent the potential complicating effects of MTX interaction with folate receptors and therefore additional effects on clearance and biodistribution patterns beyond that resulting generically from drug conjugation.

The ^{3}H-labelled dendrimers synthesised were:

G3(SPN)-$(PEG_{570})_{32}$,	100% PEGylated
G4(SPN)-$(PEG_{570})_{64}$,	
G3(SPN)-$(PEG_{570})_{8}(MTX)_{8}$,	50% PEGylated, 50% MTX
G3(SPN)-$(PEG_{1100})_{8}(MTX)_{8}$,	
G4(SPN)-$(PEG_{570})_{16}(MTX)_{16}$,	
G4(SPN)-$(PEG_{1100})_{16}(MTX)_{16}$,	
G4(SPN)-$(PEG_{2200})_{16}(MTX)_{16}$,	
G5(SPN)-$(PEG_{570})_{32}(MTX)_{32}$ and	
G5(SPN)-$(PEG_{1100})_{32}(MTX)_{32}$.	

The preparation of the dendrimers is described in detail in the supplementary information available at http://www.pubs.acs.org. The SuN$(PN)_2$ wedges were prepared according to Scheme 1. Mono-BOC-1,3-diaminopropane was mono-alkylated with N-(benzyloxycarbonyl)-3-bromopropylamine, then reacted with succinic anhydride to give the carboxylic acid. This was then protected as the ethyl ester, the Cbz group removed, and replaced with a PEG group. The BOC group was then removed and replaced by MTX(-α-OtBu)[24]. Lastly the ethyl ester was removed, and the wedge coupled to the radiolabelled dendrimer (Scheme 2).

The specific radioactivity of the dendrimers was determined by dilution of a known mass of dendrimer (in triplicate) in 1 ml Starscint, followed by scintillation counting using a Packard Tri-Carb 2000CA Liquid Scintillation Analyser (Meriden, CT). Specific activity was typically within the range of 0.5 to 1 μCi/mg.

The particle size and polydispersity index (PDI) of dendrimers with identical molecular weight, but composed of generation 4 all L-lysine (G4(Lys)-$(PEG_{570})_{32}$) or with an outer layer of $SuN(PN)_2$ (G4(SNP)-$(PEG_{570})_{32}$) were compared by photon correlation spectroscopy using a Nano ZS Zetasizer (Malvern Instruments, Worestershire, UK[25]). Dendrimers were dissolved to 1 mg/ml in isotonic saline and filtered through a 20 nm membrane (Milipore, Melbourne, Australia) prior to analysis. The refractive index for the protein standard was 1.450.

Animals

Sprague Dawley rats (SD male, 270-350 g) were supplied by Monash University (Melbourne, Victoria). Rats were maintained on a 12 hour light/dark cycle and were fed standard rodent chow prior to surgery. Food was withheld after surgery and for 8 hours post IV dose but water was available at all times.

Nude athymic rats (male, 6-7 weeks of age) and SCID mice (female, 6 weeks of age) were purchased from the Australian Research Centre (Perth, WA) and were housed in microisolators (Australian Research Centre, WA) maintained at 22 °C on a 12 hour light/dark cycle. Since the athymic rats and SCID mice were not subjected to surgical implantation of cannulae or routine blood sampling, animals were provided food and water at all times.

All animal experiments were approved by the Victorian College of Pharmacy Animal Ethics Committee, Monash University (Melbourne, Victoria).

Cell culture conditions

Walker 256 cells (rat breast carcinoma) and HT1080 cells (human adenocarcinoma) were purchased from ECACC (Salisbury, UK). Walker 256 cells

were grown in 75cm^2 flasks in medium 199 supplemented with 5% FBS, 2 mM Glutamax and 1% penicillin-streptomycin in a humidified atmosphere of 5% CO_2 and 37°C. Cells were passaged 1:4 using 0.25% trypsin-EDTA twice per week. HT1080 cells were grown in 75cm^2 flasks in MEM supplemented with 2 mM Glutamax, 1% NEAA, 10% FBS and 1% penicillin-streptomycin in a humidified atmosphere as above. Cells were passaged 1:5-6 using 0.25% trypsin-EDTA 3 times per week. Both cells lines tested negative for mycoplasma contamination.

Determination of intravenous plasma pharmacokinetics in Sprague Dawley rats

SD rats were cannulated via the right jugular vein and carotid artery under isoflurane anaesthesia as described previously[23]. After surgery, rats were transferred to metabolism cages (which allowed collection of urine and faeces), and were allowed to recover overnight prior to administration of 1 ml of dendrimer solution (in 50 mM PBS, pH 7.4) via the jugular vein to provide a final dose of 5 mg dendrimer/kg. Prior to dosing, a blank blood sample (150 µl) was collected via the carotid artery into a heparinised (10 U) Eppendorf tube. Animals were dosed with each dendrimer solution as an infusion over 1.5 min. Dendrimer remaining in the cannula at the end of the infusion was flushed through the cannula with a further 200 µl of heparinised saline (2 U heparin/ml) over 30 sec. A zero time point sample (150 µl, t=0) was immediately collected via the carotid artery cannula to facilitate estimation of Cp^0 and V_c. Further blood samples (150-200 µl) were collected at t=0, 10, 20, 30, 45, 60, 90, 120, 180, 240, 360, 480, 1440 and 1800 min and stored in heparinised (100 U) Eppendorf tubes. Additional blood samples were collected at 48, 54, 72, 78, 96, 102, 120, 126, 144, and 168 h for longer circulating dendrimers. Whole blood samples were centrifuged (3,500 × g) for 5 min to isolate plasma. Plasma samples (50-100 µl) were then mixed

with 1 ml Starscint in 6 ml scintillation vials and counted for ^{3}H-content as described above.

Urinary excretion and biodistribution of ^{3}H dendrimers in Sprague Dawley rats

Urine was collected and subsequently analysed for ^{3}H-content over time periods of 0-8, 8-24, 24-30 (or 48 for longer circulating dendrimers), 48-72, 72-96 and 96-120 (168 for longer circulating dendrimers) hours. Aliquots (100 – 200 µl) of the urine collected over these time periods were analysed for ^{3}H by mixing with 1-2 ml of Starscint and scintillation counted as described above. Total urinary output was calculated from the ^{3}H in each aliquot and the measured volume of urine collected over the collection period.

For the biodistribution studies, rats were euthanised by intravenous infusion of Lethabarb (1 ml of 325 mg/ml pentobarbitone sodium) at various times post dose depending on the timescale of circulation. Thus, animals administered G4(SPN)-$(PEG_{570})_{32}$, G3(SPN)-$(PEG_{570})_{8}(MTX)_{8}$, G3(SPN)-$(PEG_{1100})_{8}(MTX)_{8}$ and G4(SPN)-$(PEG_{570})_{16}(MTX)_{16}$ were euthanised at 30 h post dose, G5(SPN)-$(PEG_{570})_{64}$ at 78 h post dose, G4(SPN)-$(PEG_{1100})_{16}(MTX)_{16}$ at 96 h post dose, G4(SPN)-$(PEG_{2200})_{16}(MTX)_{16}$ and G5(SPN)- $(PEG_{570})_{32}(MTX)_{32}$ at 120 h post dose and G5(SPN)-$(PEG_{1100})_{32}(MTX)_{32}$ at 168 h post dose. The major organs (liver, kidneys, spleen, pancreas, heart, lungs, brain) were removed, weighed and homogenised in 5-10 ml Milli-Q water using a Waring mini-blender (Extech Equipment Pty. Ltd, Boronia, Australia) for 5 × 10 second intervals. The homogenates were processed and the ^{3}H-content of the homogenates determined as described previously[23].

Size exclusion chromatography of plasma, urine and kidney homogenate

Arterial blood and urine collected at various time points were analysed by size exclusion chromatography to identify the tritiated species present. Prior to injection onto the column (Superdex 75, Amersham Biosciences, NJ, USA) plasma and urine samples were diluted 1:1 in mobile phase (50 mM PBS + 0.3 M NaCl, pH 3.5) where tritium counts were high enough to facilitate column separation and scintillation counting of collected fractions. Sample aliquots (100-200 µl) were then injected onto the column and eluted with mobile phase at 0.5 ml/min using a Waters 590 pump (Millipore Corporation, Milford, MA, USA). Fractions were collected every 1 min using a Gilson FC10 fraction collector (John Morris Scientific Pty. Ltd., Melbourne, Australia) and mixed with 3 ml Starscint in 6 ml scintillation vials prior to scintillation counting for ^{3}H-content as described above.

Kidney homogenate (obtained from rats administered G3(SPN)-$(PEG_{570})_8(MTX)_8$, G3(SPN)-$(PEG_{1100})_8(MTX)_8$ and G4(SPN)-$(PEG_{570})_8(MTX)_8$) was also analysed by size exclusion chromatography. Approximately 1 ml of homogenate was collected into separate Eppendorf tubes and centrifuged at 10,000 × g for 5 min to remove large particulate material. The supernatant was then filtered through a 0.22 µm polypropylene membrane (13 mm filter unit, Lida Manufacturing Corp., WI, USA) to remove insoluble particles. The filtered supernatant was mixed 1:1 with mobile phase and 200 µl was injected onto the column. Fractions were collected and analysed as described above.

Tumour deposition of G5(SPN)-$(PEG_{1100})_{32}(MTX)_{32}$ in Nude rats and SCID mice

Walker 256 and HT1080 cells were used between passages 5 and 10. For induction of solid tumours in nude rats, cells were passaged using trypsin-EDTA,

washed once in HBSS and resuspended to 3×10^7 cells per ml in HBSS. A 200 µl suspension of Walker 256 or HT1080 cells (6×10^6 cells in total) was then injected into the right flank of rats (n=6-7 rats for each cell line) using a 25G needle. Tumour growth was monitored with a pair of callipers every 2 days (Equation 1 below). When tumours reached approximately 1000 mm^3 (approximately 17 days for Walker 256 tumours and 10 days for HT1080 tumours) rats were anaesthetised with 3% isoflurane and injected with 1 mg of G5(SPN)-$(PEG_{1100})_{32}(MTX)_{32}$ in a final volume of 200 µl of sterile saline intravenously via the tail vein using a 27G needle. Rats were then killed after collection of blood via cardiac puncture under isoflurane anaesthesia via direct cardiac administration of 1 ml Lethabarb 2 or 5 days after IV dosing and tumour, liver, spleen, muscle (from the left thigh) and fat (from the left dorsal region) collected for biodistribution analysis as described above.

Equation 1: $$volume(mm^2) = \frac{4}{3}\Pi(a \times b^2)$$

where a = longest radius (mm), b = shortest radius (mm)

Since tumour deposition studies are typically not conducted in rats, for comparison of tissue deposition data in rats to the more commonly used mouse model, a suspension of 1×10^7 HT1080 cells per ml of HBSS (as above) was prepared and 1 million cells (in a final volume of 100 µl) injected into the left flank of 6 mice using a 25G needle. Tumour growth was monitored every 2 days. When tumours reached approximately 100 mm^3 (Equation 1, approximately 23 days) mice were injected with 0.15 mg of G5(SPN)-$(PEG_{1100})_{32}(MTX)_{32}$ intravenously via the tail vein using a 27G needle. After 2 days, mice were injected IP with 100 µl Lethabarb and blood (via cardiac puncture) collected prior to death. Tumour, liver, spleen, pancreas, kidneys, heart, lungs, muscle (from the right thigh) and fat (from the right dorsal region) were excised after death and collected into 20 ml scintillation vials. Whole organs and

blood (100 µl) were solubilised in 4 ml of 1:1 soluene:isopropanol by overnight heating at 60°C as described previously[23]. Following tissue solubilisation, one quarter of the solubilised liver was collected into a separate tube for further analysis. Tissue samples were then bleached with 400 µl 30% hydrogen peroxide and 10 ml Starscint added, vortexed and kept at 4°C for 3 days until samples were counted on a scintillation counter.

Calculation of pharmacokinetic parameters

The amount of radiolabel in each plasma sample was converted to ng dendrimer equivalents using the specific activity of the ^{3}H-labelled dendrimer. Plasma concentrations have been expressed as ng equivalents/ml, however this should be viewed with the caveat that this approach assumes that the ^{3}H-content is still associated with intact dendrimer.

The terminal elimination rate constants (k) were obtained by regression analysis of the individual post-distributive plasma concentration *vs.* time profiles. Half lives ($t_{½}$) were determined from ln 2/k. The area under the plasma concentration *vs.* time profiles ($AUC^{0-\infty}$) were calculated using the linear trapezoidal method. The extrapolated area ($AUC^{tlast-\infty}$), was determined by division of the last measurable plasma concentration (C_{last}) by k. The initial distribution volume (V_c) was calculated by dividing the administered dose by the concentration in plasma at t=0 (C_p^{0}). Post-distributive volumes of distribution ($V_{D\beta}$) were determined by dividing the administered dose by k × $AUC^{0-\infty}$. Plasma clearance (Cl) was calculated by dose/$AUC^{0-\infty}$.

Statistics

Statistical analyses were performed using a 2-way unpaired T-test to compare the pharmacokinetic parameters calculated for dendrimers composed of $SuN(PN)_2$ and natural L-lysine, for fully PEGylated and half-drugylated dendrimers and for comparison of pharmacokinetic parameters between MTX-conjugated PEG_{570} and PEG_{1100} dendrimers (Generation 3 and 5 only). A 1-way ANOVA and Tukey's post-test were used to compare the pharmacokinetic parameters of MTX-conjugated dendrimers of differing Generation and PEG chain length for G4 dendrimers. Significance was determined at a level of $p<0.05$.

Results:

Comparison of intravenous pharmacokinetics and disposition of G4(Lys)-$(PEG_{570})_{32}$ and G4(SPN)-$(PEG_{570})_{32}$

Previous studies have reported the potential utility of poly-lysine dendrimers as drug delivery vehicles where the dendrimer scaffold was composed entirely of natural L-lysine[22, 23, 26]. To identify potential differences between PEGylated poly-L-lysine dendrimers containing an outer generation of natural L-lysine or the symmetrical analogue of lysine employed here, the IV pharmacokinetics and disposition of symmetrical G4(SPN)-$(PEG_{570})_{32}$ was compared to that of the previously reported asymmetrical (natural) G4(Lys)-$(PEG_{570})_{32}$. The two dendrimers were analogous in both molecular weight and in hydrodynamic radius as determined by photon correlation spectroscopy (Table 1). A significant difference in the plasma residence times of the two dendrimers was evident (Figure 2A, Table 1). The plasma half life of G4(SPN)-$(PEG_{570})_{32}$ (13.6 h) was significantly longer and plasma

clearance (2.7 ml/h) lower than G4(Lys)-$(PEG_{570})_{32}$ (Table 1). There were no significant differences in the distribution volumes for the two dendrimers. The urinary excretion of G4(SPN)-$(PEG_{570})_{32}$ was also lower than that of G4(Lys)-$(PEG_{570})_{32}$ (approximately 33 % vs. 43% of injected ^{3}H respectively), however this difference was not statistically significant (Table 1).

The organ distribution of G4(SPN)-$(PEG_{570})_{32}$ (30 h post dose) was similar to that of G4(Lys)-$(PEG_{570})_{32}$ (Figure 2B) and showed in general low levels of radioactivity in all organs collected. Significantly higher levels of G4(SPN)-$(PEG_{570})_{32}$ were recovered in the liver and lungs when compared to G4(Lys)-$(PEG_{570})_{32}$.

Comparison of pharmacokinetics and biodistribution of fully PEGylated and MTX conjugated dendrimers

Comparison of the plasma pharmacokinetic parameters of fully PEGylated dendrimers containing a symmetrical analogue of lysine in the outer generation (G4(SPN)-$(PEG_{570})_{32}$ and G5(SPN)-$(PEG_{570})_{64}$) with the respective half PEGylated, half 'drugylated' constructs of similar MW revealed significant differences between the IV pharmacokinetics of the two species (Figure 3). When compared with the fully PEGylated species, the more hydrophobic drug conjugated constructs show increased plasma clearance and reduced half life (Table 2 and Figure 3), although the increased clearance was not reflected in increased targeting towards reticuloendothelial (RES) organs. Indeed, the higher plasma clearance of G4(SPN)-$(PEG_{570})_{16}(MTX)_{16}$ when compared with the fully PEGylated construct appeared to result from retention of the dendrimer in the kidneys, especially for the G4 constructs.

Plasma pharmacokinetics of methotrexate conjugated dendrimers in Sprague Dawley rats

Figure 4 shows the plasma concentration-time profiles of a series of G3 (Panel A), G4 (Panel B) and G5 (Panel C) dendrimers with 50% surface coverage of different MW PEGs and 50% surface coverage of methotrexate. Across the dendrimer generations, a relationship between PEG chain length and plasma circulation time was evident, where increasing the MW of attached PEG decreased clearance and increased the elimination half life (Table 3, Figure 5). The data also suggest that systems with molecular weights less than approximately 20 kDa were cleared relatively rapidly from plasma.

For the G3 dendrimers (Figure 4A), a small increase in the plasma half life and decrease in clearance for the PEG_{1100} derived dendrimer was evident when compared with the PEG_{570} construct, however, in both cases plasma clearance and urinary elimination was relatively rapid, presumably reflecting the lower molecular weight of the G3 system (Table 3).

For the G4 dendrimers (Figure 4B) a good correlation was seen between increased PEG chain length, dendrimer molecular weight and the calculated pharmacokinetic parameters. Increasing PEG molecular weight increased dendrimer MW from 21.1 to 47.2 kDa, decreased clearance from 52 to less than 1 ml/min and in turn increased terminal half life from less than 1 h to 34 h (Table 3).

For both the G5 dendrimers clearance decreased from 1.5 to 0.6 ml/min with increased PEG chain length resulting in an increase in terminal half life from approximately 1 day to more than 2 days. For all generation dendrimers examined, PEGylation has little effect on volume of distribution.

Across the series of MTX-derived G3-G5 dendrimers examined here and including data obtained for similar fully PEGylated dendrimers previously[22], a relationship was apparent between clearance and MW (Figure 5A) and also between terminal half life and MW (Figure 5B) where pronounced reductions in clearance and increases in half life were seen for constructs where MW> 20 kDa.

Urinary excretion of MTX conjugated dendrimers

The total quantity of injected tritium recovered in urine over the 30 h sampling period was approximately 55-65% for both of the G3 dendrimers (Table 3). Whilst approximately 10% more injected radioactivity was recovered for the PEG_{1100} dendrimer this was not significantly different to the PEG_{570} dendrimer. Most (approximately 50% of the injected dose) of the radioactivity recovered in urine was excreted over the initial 8 h post-dose period (see supplementary information).

The quantity of injected ^{3}H recovered in the urine of rats administered the G4 dendrimers G4(SPN)-$(PEG_{570})_{16}(MTX)_{16}$ and G4(SPN)-$(PEG_{1100})_{16}(MTX)_{16}$ was similar (29 vs 23.5% respectively), but considerably lower than that for the G3 dendrimers with the equivalent PEG chains. There was an even clearer decrease in urinary excretion on increasing the PEG chain length on the G4 dendrimer to 2300 Da (8.4%, Table 3) possibly suggesting a threshold in the dendrimer size (>20 kDa) required to avoid urinary elimination. Similar to the G3 dendrimers, the PEG_{570} and PEG_{1100} derived G4 dendrimers were relatively rapidly excreted into urine over the first 8 h after dosing (see supplementary information). For the G5 dendrimers, very little administered ^{3}H was excreted into urine over the sampling period, presumably reflecting hindered renal filtration of the large (>40 kDa) PEGylated dendrimers.

Size Exclusion Chromatography of Plasma and Urine

For the majority of the dendrimers, intact dendrimer was the dominant species in plasma and urine (see supplementary information for SEC profiles). The only exception was in urine samples collected at later time periods from rats administered smaller dendrimers where a proportion of the radiolabel was present as low molecular weight species. The absolute quantity of radiolabel in the urine at these time points, however, was low when compared to the total proportion of the renally excreted dose.

Biodistribution of MTX conjugated dendrimers in Sprague Dawley rats

At the completion of the study major organs were collected to determine the pattern of distribution of the injected dendrimers and the results are presented as both the tissue mass corrected proportion of radiolabelled dose remaining in each tissue (left side of Figure 6) or as the total proportion of injected ^{3}H dose recovered in each organ (right side of Figure 6). Whilst uptake into the brain was analysed, the radiolabel content was below accurately quantifiable limits (less than 0.1% injected ^{3}H per g of tissue) in all cases.

For the G3 dendrimers, the majority of the remaining radiolabel was detected in the kidneys (Panels A and B). Small amounts of radiolabel were detected in other organs, however the quantity of radiolabel in these organs accounted for less than 1% of injected ^{3}H per organ (Panel B). Interestingly, almost 20% of administered G3(SPN)-$(PEG_{570})_8(MTX)_8$ was recovered in the kidneys at 30 h compared with only 2% for the larger G3(SPN)-$(PEG_{1100})_8(MTX)_8$, although similar proportions of radiolabel were excreted via the urine for both dendrimers. Size exclusion analysis of the supernatant of kidney homogenate revealed that most of the radiolabel retained in the kidneys of rats administered the G3 dendrimers was attributed to low molecular

weight breakdown products that were also identified in later (8-24h) urine samples (see supplementary information).

Slightly higher proportions of the G4 dendrimers were recovered in collected organs and in particular the liver which contained up to 10% of the administered dose at the end of the study. With the exception of G3(SPN)-$(PEG_{570})_8(MTX)_8$, roughly similar proportions of radiolabel were recovered for each dendrimer in the liver, kidneys, spleen, pancreas, heart and lungs and these accounted for ≤ 1% of the injected dose per gram of tissue. This is similar to the biodistribution pattern for the fully PEGylated G4(SPN)-$(PEG_{570})_{32}$ shown in Figure 2B. Consistent with the data obtained for the G3 PEG_{570} dendrimer, however approximately 23% of the administered dose of G4(SPN)-$(PEG_{570})_{16}(MTX)_{16}$ was recovered in the kidneys, although in this case the radioactivity could be attributed entirely to intact dendrimer by SEC (see supplementary information). The proportion of injected dose retained in the kidneys decreased sharply to less than 1% for the PEG_{1100} and PEG_{2200} derived dendrimers. The amount of radiolabel recovered in the liver and kidneys increased with increasing PEG chain length, from approximately 0.2% injected ^3H/g liver and spleen for the PEG_{570} dendrimer to approximately 1% injected ^3H/g for the PEG_{2300} dendrimer.

The proportion of the G5 dendrimers recovered in the kidneys, pancreas, heart and lungs were similar regardless of PEG chain length. Slightly higher proportions of the injected dose were recovered in the liver (10-12% of administered ^3H) and spleen (approximately 2% of administered ^3H) when compared with the G4 dendrimers (1-7% and <1% of administered ^3H for liver and spleen respectively).

Tumour Biodistribution of G5(SPN)-$(PEG_{1100})_{32}(MTX)_{32}$ in rats and mice

The tumour disposition of the largest (and longest circulating) dendrimer (G5(SPN)-$(PEG_{1100})_{32}(MTX)_{32}$) was examined in animals bearing solid rat mammary carcinomas (Walker 256) or human adenocarcinoma (HT1080). For direct comparison with the pharmacokinetic data obtained in rats, both tumours were generated in immunocompromised rats and tumour disposition analysed 2 and 5 days after an IV dose. Since the mouse model is also commonly used to study EPR of nanosized delivery constructs, the tumour distribution of G5(SPN)-$(PEG_{1100})_{32}(MTX)_{32}$ was also examined 2 days after an IV dose in mice bearing solid HT1080 tumours.

The distribution of G5(SPN)-$(PEG_{1100})_{32}(MTX)_{32}$ in rats bearing solid Walker 256 (Panel A) and HT1080 (Panel B) tumours is shown in Figure 7. Tumour accumulation of G5(SPN)-$(PEG_{1100})_{32}(MTX)_{32}$ was similar to the degree of uptake into the RES organs (approximately 1-2% per g) and was in all cases much greater (approximately 5-10 fold) than uptake into control tissues (muscle and fat). Mass normalised distribution into the Walker tumour was slightly lower than that seen in the HT1080 tumour and the amount retained (per g of tumour) decreased from 2 to 5 days. The decrease in dendrimer localisation in Walker tumours from 2 to 5 days largely reflected an increase in tumour mass since whole tissue accumulation remained at 4-5% of the injected dose. In contrast, uptake into the HT1080 tumour (per g of tumour) varied less, most likely reflecting the smaller increase in size of the HT1080 tumour from 2-5 days. The whole tissue distribution of G5(SPN)-$(PEG_{1100})_{32}(MTX)_{32}$ into HT1080 tumours was approximately 2% of the administered dose over the 3 day period.

The disposition of G5(SPN)-$(PEG_{1100})_{32}(MTX)_{32}$ in mice bearing HT1080 tumours is shown in Panel C. Uptake into the HT1080 tumour in mice was relatively effective (11% dose per g) and the construct accumulated to a similar extent in the tumour and spleen. Tumour uptake was approximately 5-10 fold more effective than uptake into muscle or fat in close agreement with the rat data.

The mass normalised distribution of G5(SPN)-$(PEG_{1100})_{32}(MTX)_{32}$ into mouse tissues was generally 10 fold higher than that in the rat, reflecting the approximately 10 fold smaller body mass of mice vs rats (although in the case of uptake into the liver the increase in the mouse was only approximately 3 fold). The whole tissue distribution of G5(SPN)-$(PEG_{1100})_{32}(MTX)_{32}$ into liver and spleen were also lower in the mouse than in the rat model (see supplementary information), but the absolute extent of accumulation of the dendrimer into HT1080 tumour was the same in both species (see supplementary information).

Discussion:

Previous reports describing the pharmacokinetic behaviour of PEGylated poly-L-lysine dendrimers have suggested that they may be used to target anticancer drugs to solid tumours and to avoid or reduce accumulation in RES organs[20]. The majority of the initial studies in this area, however, have been undertaken with PEGylated dendrimers and the potential impact of surface derivatisation of drug has been less well defined. The current study was therefore undertaken to characterise the changes in the biopharmaceutical profile of PEGylated poly-lysine dendrimers after replacement of 50% of the surface PEG groups with a model hydrophobic drug (methotrexate) and to further examine the capacity of these systems to promote

extended circulation times and tumour uptake in rats and mice. In these studies the outer generation of the polylysine dendrimers was composed of a symmetrical analogue of lysine ($SuN(PN)_2$) in an attempt to enhance plasma circulation time. A fully PEGylated G4 dendrimer containing an outer $SuN(PN)_2$ layer was therefore initially compared with data obtained for a similar construct containing natural L-lysine in the outer layer. The dendrimer constructed with the $SuN(PN)_2$ wedge was cleared more slowly than the natural analogue (Figure 2), although the dendrimers ultimately showed similar organ deposition profiles. The slower plasma clearance of the $SuN(PN)_2$ dendrimer appeared, at least in part, to result from decreased renal excretion, although this difference was not statistically significant. We have previously reported that the plasma clearance of PEGylated dendrimers is closely related to the extent of renal elimination which in turn is a function of molecular weight[22]. The molecular weights and hydrodynamic radii of the dendrimers generated using $SuN(PN)_2$ and L-lysine, however, were similar. An explanation for the less avid renal clearance of the $SuN(PN)_2$ derived dendrimers is therefore not clear at this time, but may suggest that the symmetrical dendrimers are less flexible than dendrimers composed of all L-lysine. Structural flexibility has previously been identified to impact upon renal and therefore plasma clearance since more flexible structures (such as linear polymers) can conform to fit through glomerular filtration slits, whereas the filtration of more rigid, globular structures with identical molecular weights is more hindered[27]. Alternatively, the inclusion of the symmetrical $SuN(PN)_2$ may have resulted in a change to the orientation of the attached PEG layer, in turn leading to differences in renal clearance.

Having demonstrated that the circulation time of fully PEGylated poly lysine dendrimers may be enhanced by the utilisation of a symmetrical analogue of lysine in

the terminal layer, subsequent studies explored the impact of the replacement of 50% of the surface PEG chains with a model hydrophobic drug, in this case, methotrexate. In general, replacement of 50% of the surface PEG groups with the MTX increased plasma clearance and decreased circulatory half life (Table 2, Figure 3) even though molecular weight remained relatively constant. In the case of the G4 dendrimers, the increase in clearance appeared to result largely from extensive retention of G4(SPN)-$(PEG_{570})_{16}(MTX)_{16}$ in the kidneys. For the G5 dendrimers, the most significant difference in biodistribution between the two dendrimers was greater uptake of the drug-conjugated dendrimer into the spleen. Removal of 50% surface PEG and substitution with acetyl groups (rather than MTX) has previously been shown to result in substantially increased plasma clearance of PEGylated polylysine dendrimers[25]. In this case, however, differences could be attributed to a large reduction in MW and increase in renal clearance.

Substitution of surface PEG with MTX therefore increased plasma clearance, however construction of dendrimers with a natural (asymmetrical) lysine surface layer rather than ($SuN(PN)_2$) helped to off-set this increase in clearance. A larger range of 50% PEG/50% MTX conjugates were therefore generated employing the symmetrical $SuN(PN)_2$ surface in order to better define the impact of drug conjugation on clearance and deposition.

Across the expanded series of 50% PEG, 50% MTX constructs, increasing the core size from G3 to G5 or increasing the PEG chain length increased the terminal half life and reduced clearance in all cases (Table 3, Figure 4). Interestingly, the relationship between the molecular weight of the construct and changes to clearance and half life were similar to that seen previously with fully PEGylated natural lysine systems, with the exception that for the partly ‘drugylated’ systems, slightly higher

plasma clearance was seen when compared with similar sized fully PEGylated natural lysine systems (Figure 5). Approximately 10% of the large (up to 59 kDa) MTX-conjugated dendrimers was recovered in the liver and spleen at the end of the experiment, however, RES targeting was lower with the smaller (G3 and G4) dendrimers and significantly lower than that reported previously for non-PEGylated PAMAM dendrimers[28] and anionic PLL dendrimers[26]. In general, small MW products were not evident in plasma samples obtained from animals dosed with the larger MTX-PEG dendrimers and those systems modified with higher molecular weight PEG chains suggesting that increased generation and PEG chain length confers improved plasma and enzymatic stability properties. Small MW products were, however, identified in urine and kidney homogenate from rats administered the G3 dendrimers. Estimation of the proportion of the tritium dose that was recovered in urine and kidney homogenate as low MW metabolites reveals that approximately 24, 14 and 5% of the tritium dose from G3(SPN)-$(PEG_{570})_8(MTX)_8$, G3(SPN)-$(PEG_{1100})_8(MTX)_8$ and G4(SPN)-$(PEG_{570})_{16}(MTX)_{16}$ dosed rats was recovered as metabolites in the urine and kidney respectively (estimated based on total radiolabel recovery and SEC profiles of urine and kidney homogenate as described in the supplementary information). This represents a decrease in apparent metabolism by approximately 10% for each 5 kDa increase in MW. This may reflect either reduced affinity for enzymes or reduced distribution into cells and tissues that degrade poly-lysine dendrimers. It is interesting to note, however, that no evidence of metabolism was reported previously for fully PEGylated systems where the PEG chains were conjugated to an outer layer of natural lysine surface dendrimers[22].

For the purposes of the current investigation, attempts were made to reduce the capacity of the MTX-conjugated dendrimers to bind folate transport proteins (such as

the folate receptor and the reduced folate carrier) via OTBu protection of the α-carboxyl group of methotrexate. Previous studies have shown that conjugation of large molecules or protecting groups to the alpha-carboxyl group of methotrexate greatly reduces the capacity of the antifolate to bind to folate receptors[29], inhibit dihydrofolate reductase activity[30] and inhibit the growth of cancer cells[30] in contrast to conjugation via the gamma-carboxyl group, which does not appear to greatly affect folate binding affinity and anti-tumour activity when compared to methotrexate. Methotrexate was therefore conjugated to the dendrimer surface via the gamma-carboxyl and the alpha carboxyl was *tert*-butylated in order to reduce the folate binding capacity. Despite capping the α-carboxyl group, however, the 50% MTX/50% PEG_{570} G3 and G4 dendrimers were retained in the kidneys in much higher quantities than the corresponding 100% PEG constructs (approximately 10 fold higher for the G4 construct) suggesting a specific and potentially drug related mechanism of interaction for the smaller dendrimers conjugated with the lowest MW PEG. Interestingly, for the G3 dendrimer most of the radiolabel retained in the kidney was associated with a low MW species that was presumably a breakdown product of the dendrimer, whereas radiolabel retained in the kidneys after administration of the larger G4 dendrimer was associated almost entirely with intact dendrimer. In the kidneys, methotrexate is excreted by passive filtration and active secretory processes that involve several folate and non-folate transporters[31]. Methotrexate is also actively reabsorbed in a saturable manner within the proximal tubules by folate-binding proteins and the organic anion transporter OAT-K1[31]. A clear explanation for the unusual observations regarding uptake into the kidneys is not apparent at this time, particularly since significant uptake and potential breakdown in the kidneys has not been previously reported for similar macromolecular constructs comprising dextran-

methotrexate[10]. However it is possible that the alpha-carboxyl protection employed here may not have been sufficient to completely block the interaction of the MTX group with folate receptors. In combination with relatively short PEG chains (570 Da) this may have allowed the dendrimer or its breakdown products to become entrapped within the kidneys by binding to transporters involved with active secretion or reabsorption of antifolates. This effect is not evident in systems with higher generation dendrimers or longer PEG chains, presumably as a result of reduced interaction with folate related receptors or limited initial renal filtration. To this point, however, it is unclear why the renal uptake of ^{3}H for the G3, PEG_{570}-MTX system was associated with smaller breakdown products whereas the high quantities of radiolabel present in the kidneys after administration of the G4 PEG_{570}-MTX system is largely associated with intact dendrimer. Studies are ongoing to examine these issues in more detail.

The final aim of the current study was to investigate the potential for PEGylated PLL dendrimers to deliver hydrophobic anticancer drugs to solid tumours in mice and rats via the EPR effect. To our knowledge this is one of the first direct comparisons of tumour targeting in rats and mice and provides interesting insight into the pattern of deposition of macromolecular constructs across the two commonly used species.

The HT1080 tumour deposition data for G5(SPN)-$(PEG_{1100})_{32}(MTX)_{32}$ in mice and rats showed approximately 5 to 10 times higher accumulation in tumour tissues when compared with control tissues (fat and muscle). The extent of tumour deposition of the MTX-conjugated dendrimer in mice (approximately 10%/g tumour) was consistent with previous mouse deposition data reported by Lee and colleagues for much larger polyester dendrimers conjugated with 50% PEG and 50% doxorubicin

in a C26 tumour model (approximately 10-15, 6-10 and <1%/g for C26 tumour, RES organs and fat and muscle respectively)[12]and by Lim et al for several PEGylated triazine dendrimers in PC3 tumours (approximately 5-8%/g). In the rat model the pattern of biodistribution was similar to the mouse, with approximately 5-10 times higher accumulation of the dendrimer into both Walker and HT1080 tumours when compared with fat and muscle, although in the rat a higher proportion of the absolute dose was distributed to the RES organs. The extent of dendrimer uptake into mouse tissues when expressed as the % dose/g tissue was approximately 10 fold higher than in the rat, however, this does not reflect more effective targeting but rather the smaller weight of organs in mice vs rats. Thus, 11% of the injected dose was recovered per gram in HT1080 tumours in mice when compared to 1-2% injected dose/g in rats, but in both cases this corresponded to the accumulation of approximately 2.3% of the dose in the total HT1080 tumour mass. In the larger Walker tumours a larger absolute extent of tumour accumulation was evident (4-5% of the dose), but this was again consistent with the uptake of approximately 1-2% of the injected dose per g of tumour. The current data therefore suggest that rats are an appropriate model for investigating tumour deposition of drugs and drug carrier systems and that comparable data to that generated in mice can be obtained. Rats have the additional advantage that multiple blood samples can be collected providing more reproducible pharmacokinetic and biodistribution data.

In summary, conjugation of the hydrophobic drug methotrexate to 50% of the surface of partly-PEGylated poly-lysine dendrimers increased plasma clearance, but this was attenuated by conjugation of PEG and drug to a symmetrical analogue of lysine ($SuN(PN)_2$) in the outer layer of the dendrimer. Methotrexate binds folate receptors and reduced folate carriers on many tissues and the methotrexate moiety

used here was protected at the α-carboxyl group in an attempt to avoid this specific interaction. However, it appeared that interaction with folate receptors was not completely prevented for dendrimers with shorter (570 Da) PEG chains, since extensive retention occurred in the kidneys for the G3 and G4-PEG_{570} dendrimers. In general, increasing dendrimer generation and/or PEG MW decreased plasma clearance, increased metabolic stability and decreased renal elimination across the dendrimer series. Finally, significant tumour deposition (up to 10 fold higher than control tissues) was also demonstrated for the largest 59 kDa dendrimer in both rats and mice, providing preliminary data to support the use of partly PEGylated PLL dendrimers as vectors for tumour targeting.

Acknowledgements: LMK was supported by an NHMRC Australian Biomedical Training Fellowship. EDW was supported by an NHMRC CDA. This work was supported by an ARC Linkage grant.

Supporting Information: This information is available free of charge via the Internet at http://pubs.acs.org.

Table 1. Comparison of plasma pharmacokinetics of G4(Lys)-$(PEG_{570})_{32}$ and G4(SPN)-$(PEG_{570})_{32}$ following IV dosing at 5 mg/kg in rats. Values represent mean ± s.d., n=3. ** $p<0.01$, ***$p<0.001$ *cf.* Lys dendrimer. Values for G4(Lys)-$(PEG_{570})_{32}$ are reproduced from a previous publication[22]. Hydrodynamic radius and PDI (parentheses) were estimated by photon correlation spectroscopy.

	Radius (nm)	$t_{½}$ (h)	V_c (ml)	$V_{D\beta}$ (ml)	Cl (ml/h)	% ^{3}H dose excreted in urine
G4(SPN)-$(PEG_{570})_{32}$	5.1 (0.209)	13.6 ± 0.3	13.8 ± 0.6	52.2 ± 4.5	2.7 ± 0.2	32.7 ± 7.8
G4(Lys)-$(PEG_{570})_{32}$	5.6 (0.179)	9.5 ± 0.3***	14.8 ± 0.4	65.6 ± 9.1	4.8 ± 0.6**	42.9 ± 2.6

Table 2. Plasma pharmacokinetic parameters of G4 and G5 dendrimers possessing an outer surface of $SuN(PN)_2$ wedges containing 100% PEG_{570} or 50% PEG_{570}/50% MTX following IV dosing at 5 mg/kg to rats. Values represent mean ± s.d., n=3-4. * $p<0.05$, ** $p<0.01$, *** $p<0.001$ *cf.* fully PEGylated dendrimer.

	MW (kDa)	$t_{½}$ (h)	V_c (ml)	$V_{Dβ}$ (ml)	Cl (ml/h)	% ^{3}H dose excreted in urine
Generation 4						
$(PEG_{570})_{32}$	22.2	13.6 ± 0.3	13.8 ± 0.9	52.2 ± 3.2	2.7 ± 0.1	32.7 ± 7.8
$(PEG_{570})_{16}$ $(MTX)_{16}$	21.1	0.4 ± 0.0***	23.3 ± 1.4***	32.8 ± 4.4**	51.9 ± 2.3***	29.0 ± 3.4
Generation 5						
$(PEG_{570})_{64}$	47.5	37.2 ± 1.7	13.0 ± 0.6	22.4 ± 1.1	0.4 ± 0.0	5.7 ± 0.5
$(PEG_{570})_{32}$ $(MTX)_{32}$	42.2	23.7 ± 6.2*	16.2 ± 0.1***	52.1 ± 16.4*	1.5 ± 0.1***	2.4 ± 0.5**

Table 3. Pharmacokinetic parameters of partly PEGylated dendrimers conjugated with 50% MTX following IV dosing at 5 mg/kg to rats. Values represent mean ± s.d., n=3-4.

	MW (kDa)	$t_{½}$ (h)	V_c (ml)	$V_{Dβ}$ (ml)	Cl (ml/h)	% ^{3}H dose excreted in urine
G3(SPN) $(MTX)_8$						

$(PEG_{570})_8$	10.5	0.1 ± 0.0	16.2 ± 0.7	28.4 ± 4.7	133 ± 19	55.7 ± 8.6
$(PEG_{1100})_8$	14.8	0.2 ± 0.01	19.6 ± 6.1	25.9 ± 7.0	98.5 ± 29.3	64.1 ± 4.7
G4(SPN) $(MTX)_{16}$						
$(PEG_{570})_{16}$	21.1	0.4 ± 0.0[d]	23.3 ± 1.4[a]	32.8 ± 4.4	51.9 ± 2.3[a]	29.0 ± 3.4[a]
$(PEG_{1100})_{16}$	29.6	21.0 ± 1.9[ac]	14.4 ± 1.7	41.7 ± 4.8	1.4 ± 0.1[a]	23.5 ± 17.7[a]
$(PEG_{2200})_{16}$	47.2	34.1 ± 1.3[cd]	13.3 ± 0.6[cd]	29.5 ± 2.7[ad]	0.6 ± 0.1[cd]	8.4 ± 1.4[d]
G5(SPN) $(MTX)_{32}$						
$(PEG_{570})_{32}$	42.2	23.7 ± 6.2[ab]	16.2 ± 0.1[b]	52.1 ± 16.4	1.5 ± 0.1[ab]	2.4 ± 0.5[ab]
$(PEG_{1100})_{32}$	59.2	51.3 ± 3.2[abc]	16.0 ± 1.1	43.1 ± 1.5[a]	0.6 ± 0.0[ac]	1.2 ± 0.1[abc]

[a] significant difference ($p<0.05$) *cf.* equivalent G3 dendrimer
[b] significant difference ($p<0.05$) *cf.* equivalent G4 dendrimer
[c] significant difference ($p<0.05$) *cf.* equivalent Generation PEG_{570} dendrimer
[d] significant difference ($p<0.05$) *cf.* equivalent Generation PEG_{1100} dendrimer

Scheme legends:

Scheme 1. i. **1** with N-(Benzyloxycarbonyl)-3-bromopropylamine in TEA/DMF; ii. **2** with succinic anhydride in toluene to give **3a**; iii. **3a** with DCC and DMAP in DCM/EtOH to give **3b**; iv. **3b** with ammonium formate and Pd/C in DMF/water to give **4a**; v. **4a** with PEG-NHS ester in TEA/DCM to give **4b**; vi. **4b** in TFA/DCM to

give **5a**; vii. **5a** with MTX(-α-OtBu), DIPEA, and pyBOP in DMF to give **5b**; viii **5b** with NaOH in THF/water to give **5c**.

Scheme 2. i. **1** with $SuN(PN)_2$ (PEG_{570})(MTX-α-OtBu) wedge, DIPEA, and pyBOP in DMF to give **2.**

Figure Legends:

Figure 1. Schematic diagram of poly-L-lysine dendrimers comprising 50% PEG (P) and 50% MTX linked to surface amine residues (M) associated with $SuN(PN)_2$ (SPN) groups in the outer layer (**A**) and of surface SPN(PEG)(MTX) units linked to G2-4 polylysine scaffolds (producing dendrimers of generation 3-5, **B**).

Figure 2. Plasma concentration-time profile of G4(Lys)-$(PEG_{570})_{32}$ (closed symbols) and G4(SPN)-$(PEG_{570})_{32}$ (open symbols) following 5 mg/kg IV administration to rats (**Panel A**). Distribution of injected ^{3}H 30 h after IV administration of G4(Lys)-$(PEG_{570})_{32}$ (closed bars) and G4(SPN)-$(PEG_{570})_{32}$ (open bars) (**Panel B**). Data represent mean ± s.d. (n=3). * $p<0.05$ cf. 'symmetrical' dendrimer. Data for G4(Lys)-$(PEG_{570})_{32}$ are reproduced from a previous publication.[22]

Figure 3. Plasma concentration-time profiles (**Panels A and B**) and tissue distribution (**Panels C and D**) in rats administered 5 mg/kg of G4 (**Panels A and C**) or G5 (**Panels B and D**) PLL dendrimers containing outer $SuN(PN)_2$ wedges containing 100% PEG_{570} (closed symbols) or 50% PEG_{570}/50% MTX (open symbols). Data represent mean ± s.d. (n=3-4).

Figure 4. Plasma concentration-time profiles of G3 (**Panel A**), G4 (**Panel B**) and G5 (**Panel C**) MTX conjugated dendrimers. Attached PEG groups are PEG_{570} (closed circles), PEG_{1100} (open circles) and PEG_{2200} (closed triangles). Data represent mean ± s.d. (n=3-4).

Figure 5. Correlation between dendrimer MW and plasma clearance (Panel A) and terminal half life (Panel B) for G3-G5 MTX-conjugated dendrimers containing an outer generation of $SuN(PN)_2$ (closed symbols) and similar fully-PEGylated dendrimers comprising an all L-lysine outer generation (open symbols, reproduced from Kaminskas et al, 2008[22]). MW was determined by mass spectrometry as shown in the supplementary information. Data represent mean ± s.d. (n=3-4).

Figure 6. Distribution of injected ^{3}H in major organs 30-168 hours after intravenous administration of MTX conjugated ^{3}H-dendrimers (5 mg/kg) to rats. **Panel A -** mass normalised % of injected radiolabel retained in each organ 30 h after administration of G3 dendrimers. **Panel B** - % of injected radiolabel retained in each organ 30 h after administration of G3 dendrimers. **Panel C -** mass normalised % of injected radiolabel retained in each organ 30, 96 or 120 h after administration of G4, PEG_{570}, PEG_{1100} or PEG_{2300} dendrimers respectively. **Panel D** - % of injected radiolabel retained in each organ 30, 96 or 120 h after administration of G4, PEG_{570}, PEG_{1100} or PEG_{2300} dendrimers respectively. **Panel E -** mass normalised % of injected radiolabel retained in each organ 120 or 168 h after administration of G5, PEG_{570} or PEG_{1100} dendrimers respectively. **Panel F** - % of injected radiolabel retained in each organ 120 or 168 h after administration of G5, PEG_{570} or PEG_{1100} dendrimers respectively. Black bars represent data for PEG_{570} dendrimers, white bars depict data for PEG_{1100} dendrimers and grey bars represent data for the PEG_{2300} dendrimer. Data are represented as mean ± s.d. (n=3-4).

Figure 7. Distribution of G5(SPN)-$(PEG_{1100})_{32}(MTX)_{32}$ 2 days (closed bars) or 5 days (open bars) after IV administration to athymic nude rats bearing solid Walker 256 (**Panel A**) or HT1080 (**Panel B**) tumours or in mice bearing HT1080 tumours (**Panel C**). Data are expressed as mean ± s.d. (n=3) of the % injected dose per g tissue. Rats received an IV dose when tumour reached approximately 1000 mm^3 and mice received an IV dose when tumours reached approximately 100 mm^3.

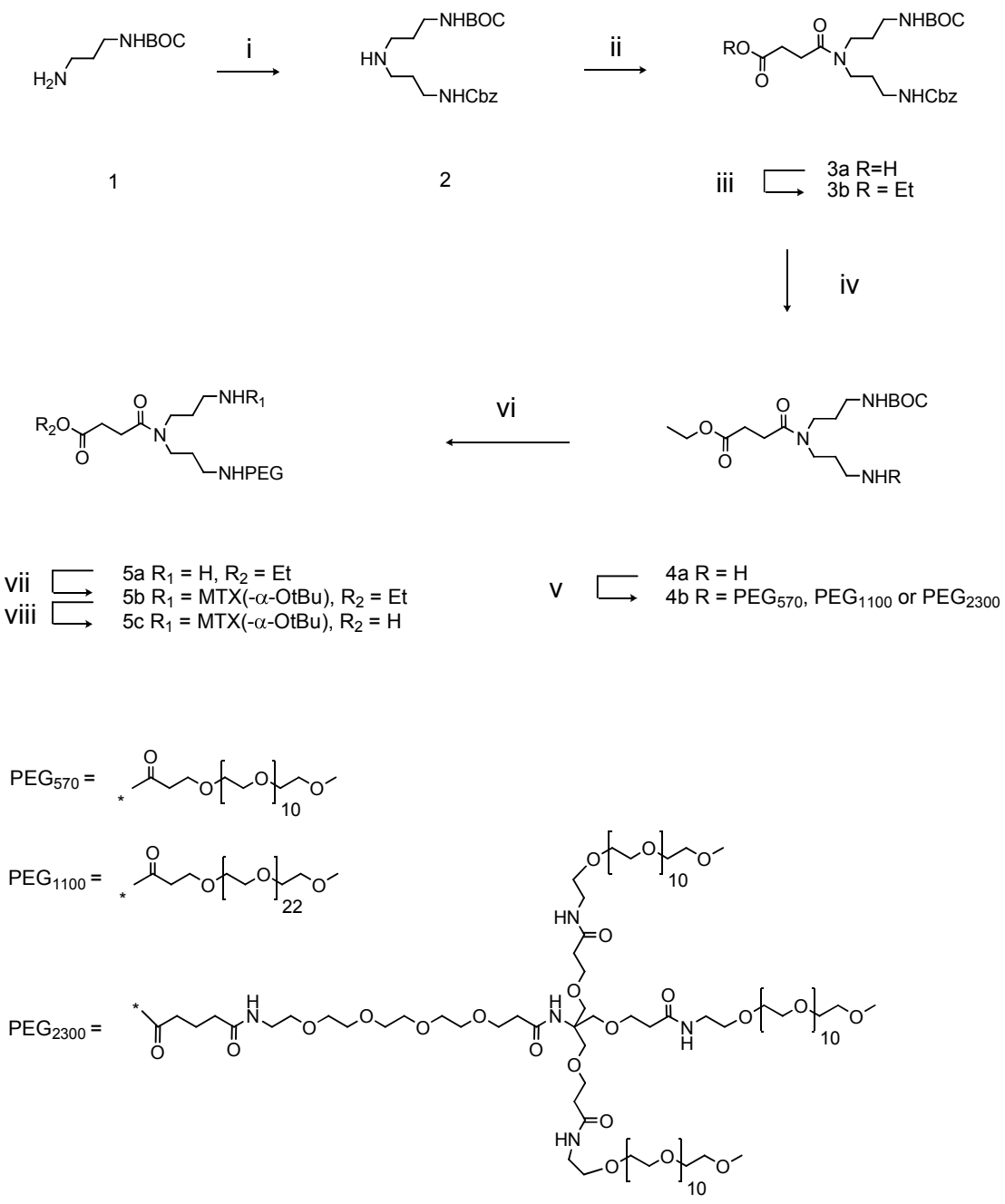
NHBOC
H_2N
i
NHBOC
HN
NHCbz
ii
RO
O
O
N
NHBOC
NHCbz
1
2
iii
3a R=H
3b R = Et
iv
vi
R_2O
O
O
N
NHR_1
NHPEG
O
O
N
NHBOC
NHR
vii
viii
5a R_1 = H, R_2 = Et
5b R_1 = MTX(-α-OtBu), R_2 = Et
5c R_1 = MTX(-α-OtBu), R_2 = H
v
4a R = H
4b R = PEG_{570}, PEG_{1100} or PEG_{2300}
PEG_{570} =
PEG_{1100} =
PEG_{2300} =
10
22
HN
O
N
H

Scheme 1

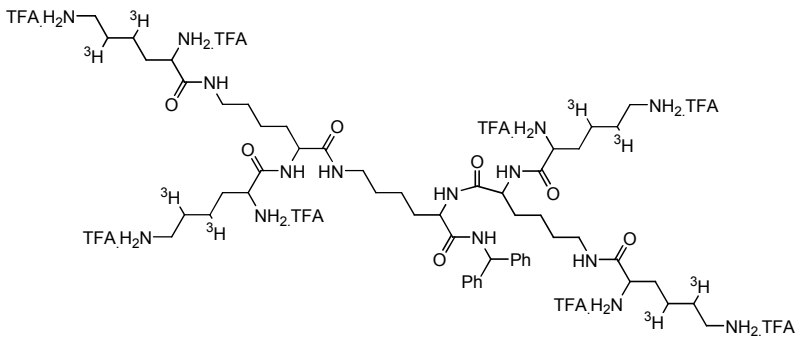

1 BHALys[Lys][Lys]$_2$[^{3}H-Lys]$_4$[TFA]$_8$

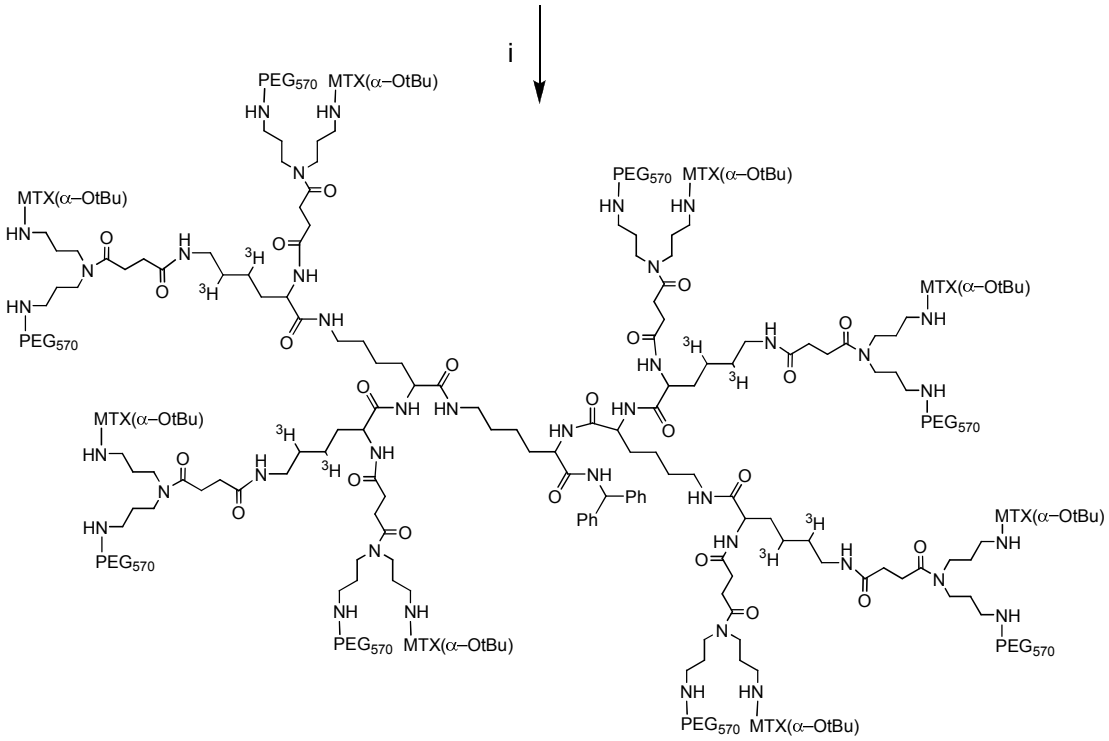

2 BHALys[Lys][Lys]$_2$[^{3}H-Lys]$_4$[SuN(PN)$_2$(PEG$_{570}$)(MTX-α-OtBu)]$_8$

Scheme 2

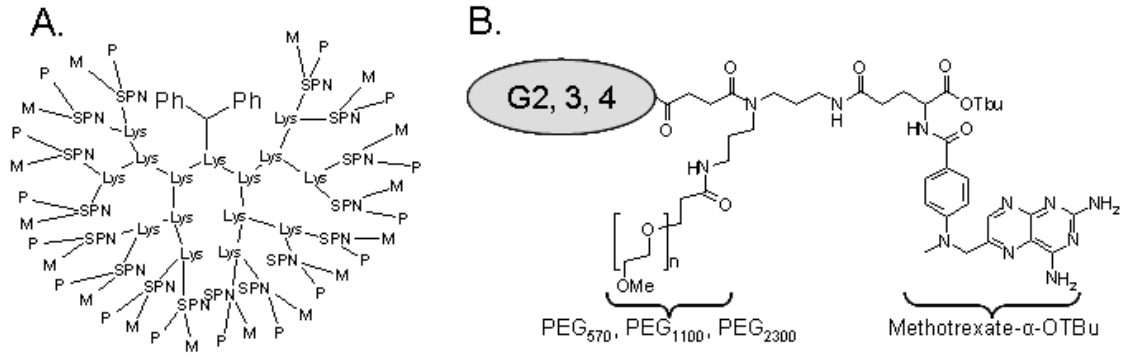
A.
B.
G2, 3, 4
OTbu
OMe
PEG570, PEG1100, PEG2300
Methotrexate-α-OTBu

Figure 1

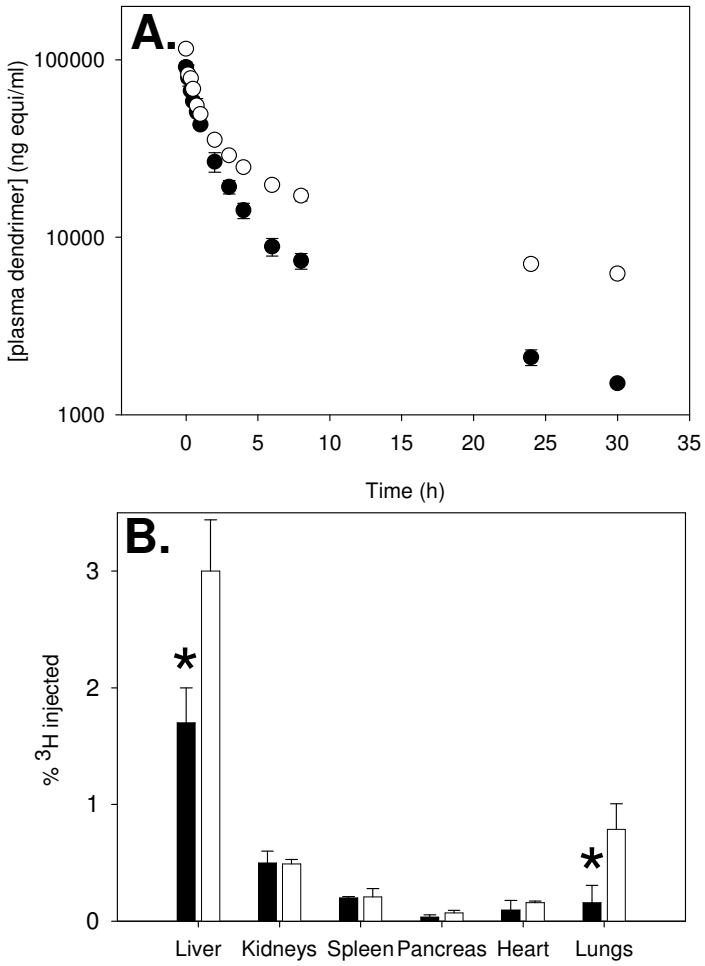
A.
[plasma dendrimer] (ng equi/ml)
100000
10000
1000
0
5
10
15
20
25
30
35
Time (h)
B.
% 3H injected
3
2
1
0
*
*
Liver
Kidneys
Spleen
Pancreas
Heart
Lungs

Figure 2

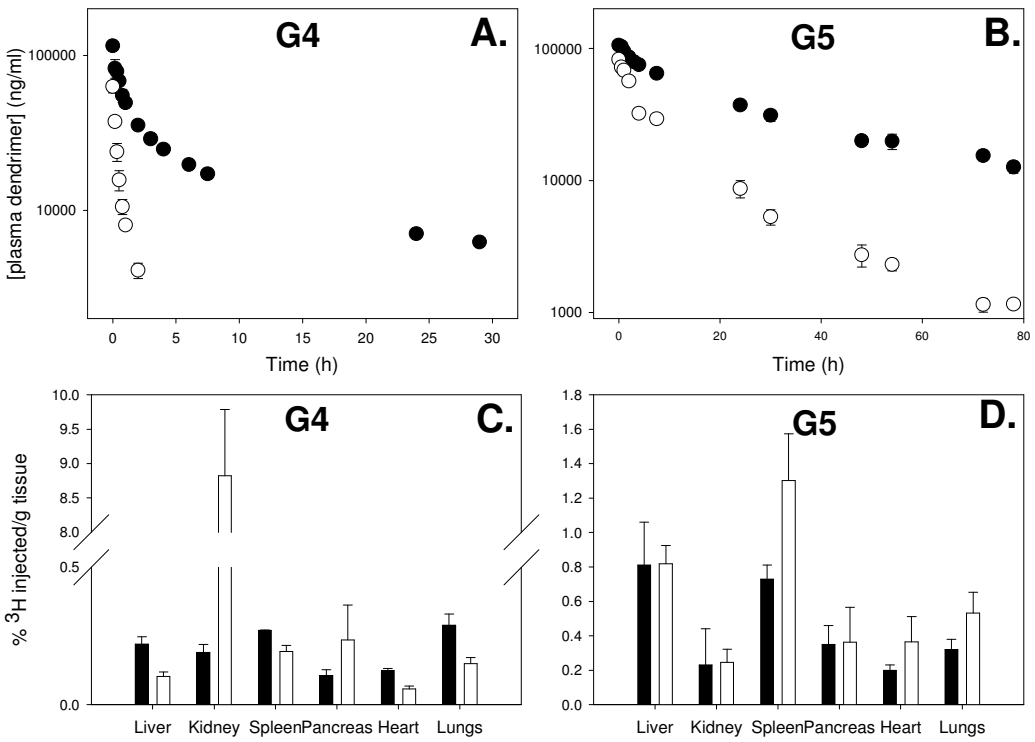
G4
A.
[plasma dendrimer] (ng/ml)
100000
10000
0
5
10
15
20
25
30
Time (h)
G5
B.
100000
10000
1000
0
20
40
60
80
Time (h)
G4
C.
% 3H injected/g tissue
10.0
9.5
9.0
8.5
8.0
0.5
0.0
Liver
Kidney
Spleen
Pancreas
Heart
Lungs
G5
D.
1.8
1.6
1.4
1.2
1.0
0.8
0.6
0.4
0.2
0.0
Liver
Kidney
Spleen
Pancreas
Heart
Lungs

Figure 3

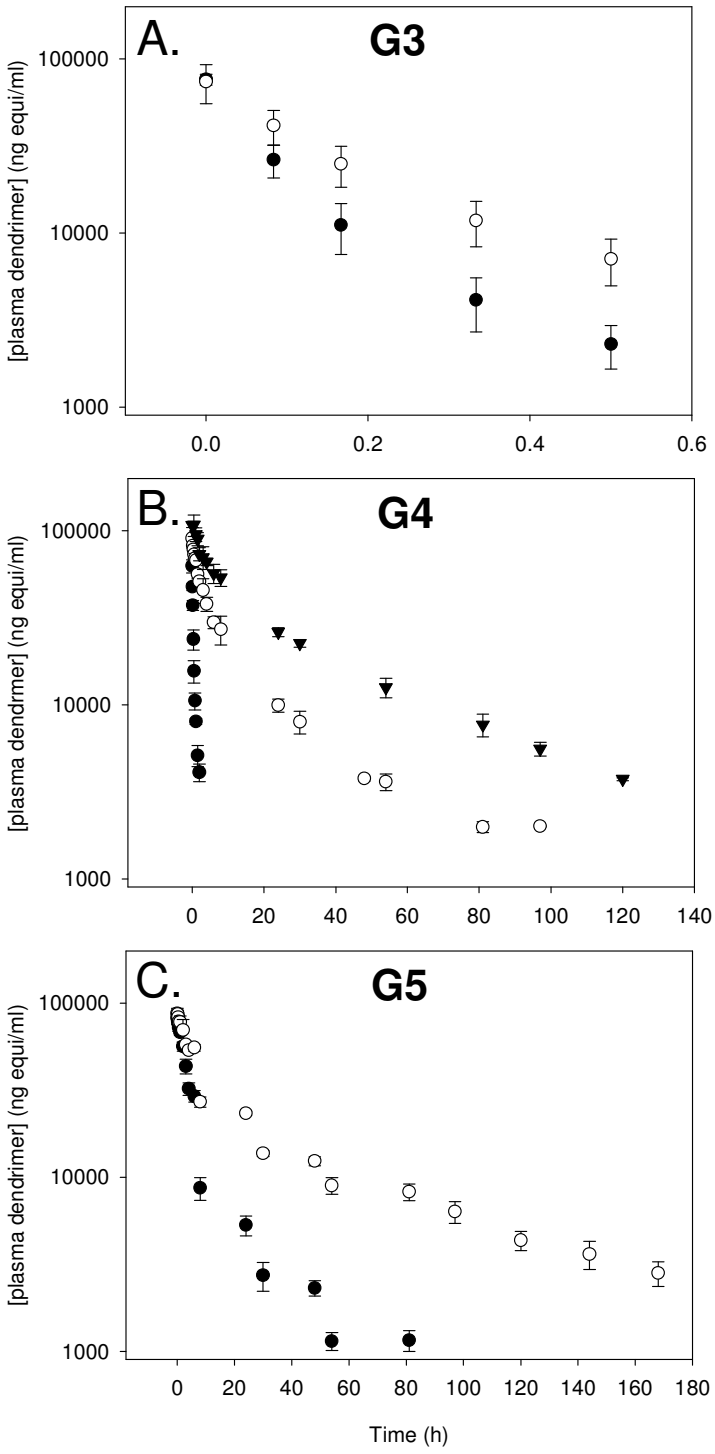
A.
G3
[plasma dendrimer] (ng equi/ml)
100000
10000
1000
0.0
0.2
0.4
0.6
B.
G4
[plasma dendrmer] (ng equi/ml)
100000
10000
1000
0
20
40
60
80
100
120
140
C.
G5
[plasma dendrimer] (ng equi/ml)
100000
10000
1000
0
20
40
60
80
100
120
140
160
180
Time (h)

Figure 4

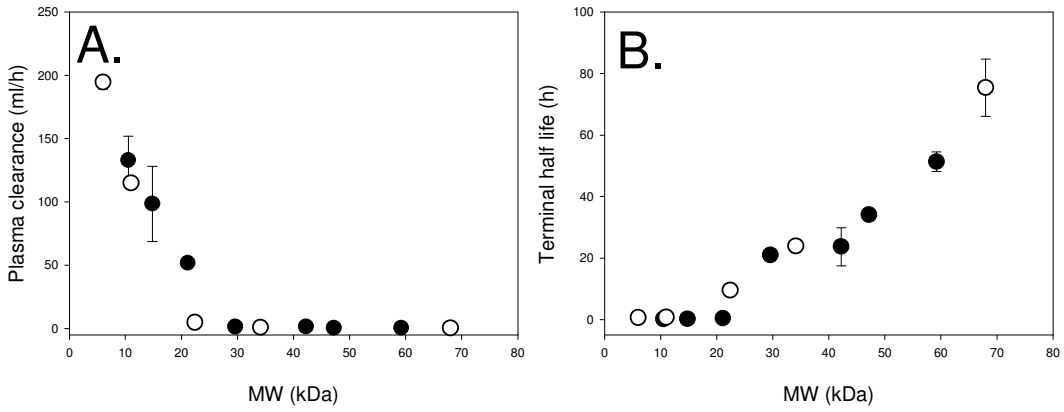

Figure 5

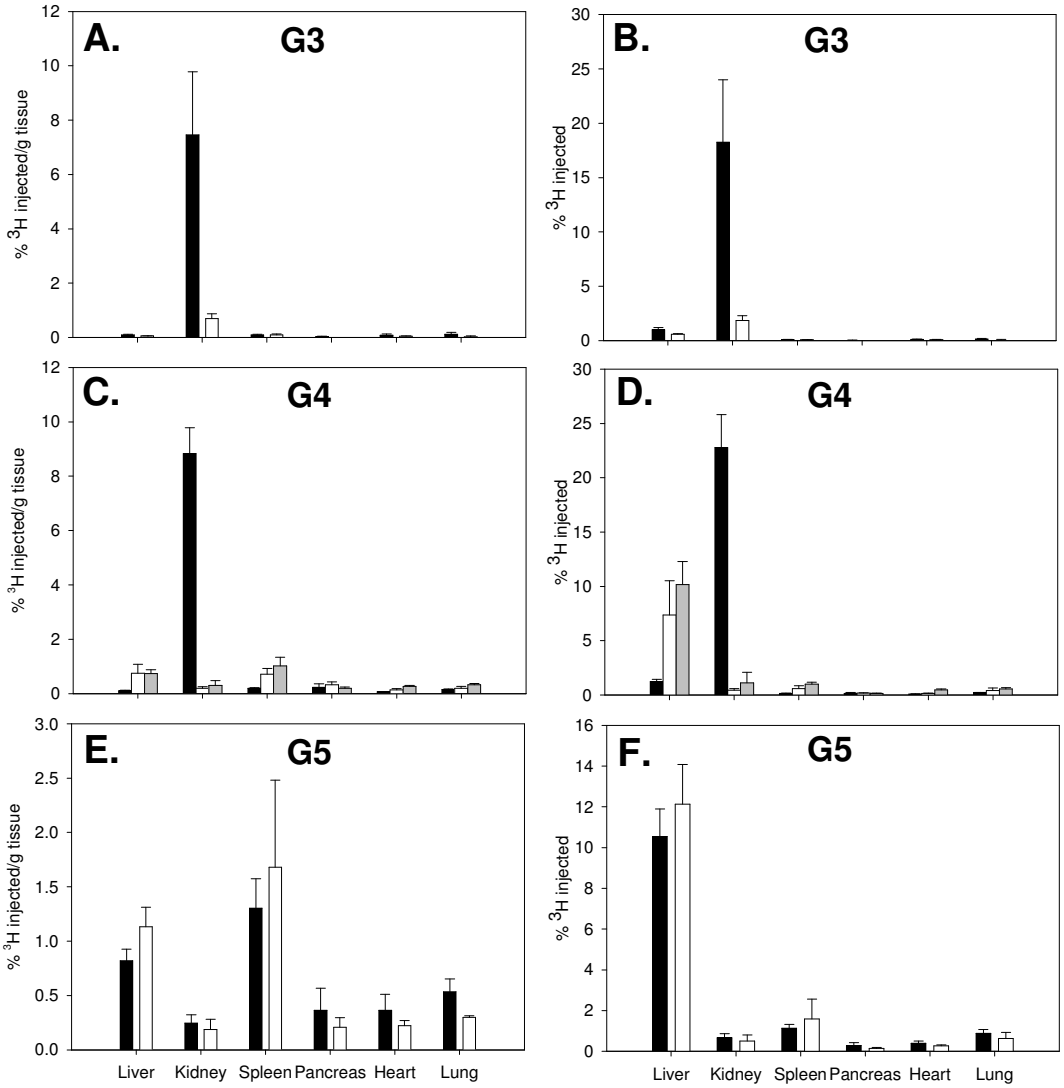
A.
G3
% 3H injected/g tissue
B.
G3
% 3H injected
C.
G4
% 3H injected/g tissue
D.
G4
% 3H injected
E.
G5
% 3H injected/g tissue
F.
G5
% 3H injected
Liver
Kidney
Spleen
Pancreas
Heart
Lung

Figure 6

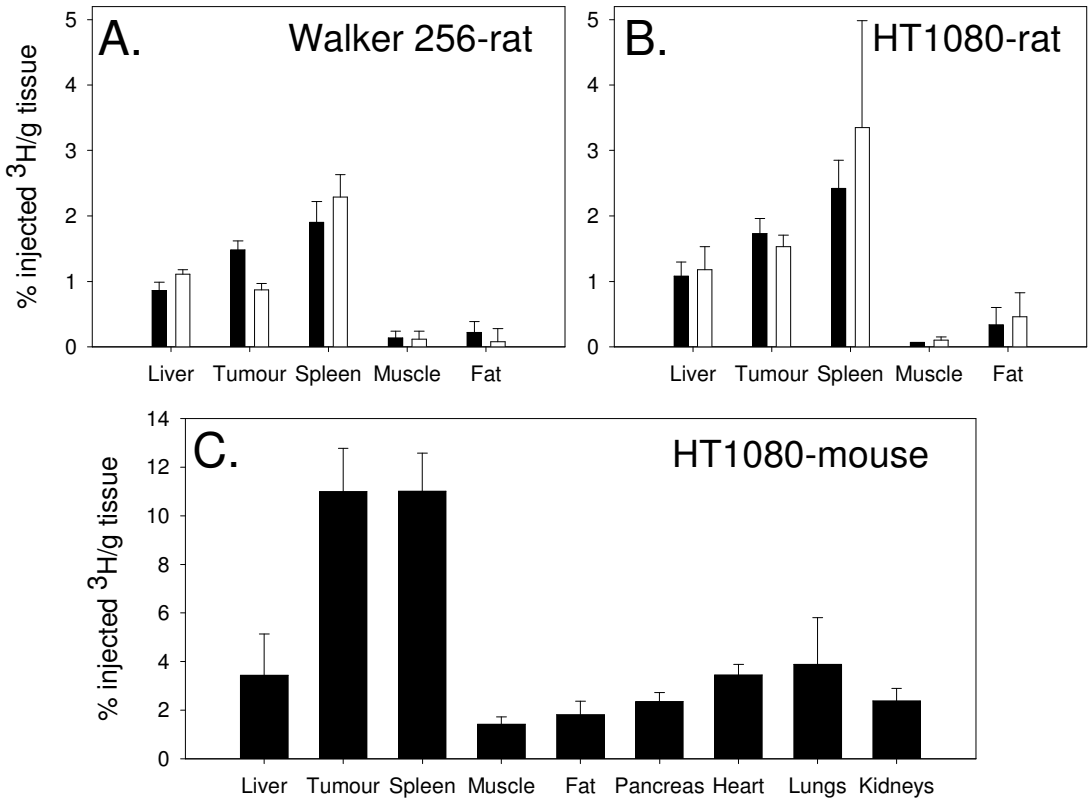
A.
Walker 256-rat
B.
HT1080-rat
C.
HT1080-mouse
% injected 3H/g tissue
Liver
Tumour
Spleen
Muscle
Fat
Pancreas
Heart
Lungs
Kidneys

Figure 7

References

1. Read T.A.; Thorsen F.; R., B. Localised delivery of therapeutic agents to CNS malignancies: old and new approaches. *Curr Pharm Biotechnol.* **2002,** 3, 257-273.
2. Albrecht, H.; DeNardo, S. J. Recombinant antibodies: from the laboratory to the clinic. *Cancer Biother Radiopharm.* **2006,** 21, 285-304.
3. Iyer, A. K.; Khaled, G.; Fang, J.; Maeda, H. Exploiting the enhanced permeability and retention effectfor tumor targeting. *Drug Disc. Today.* **2007,** 11, 812-818.
4. Portney, N.; Ozkan, M. Nano-oncology: drug delivery, imaging and sensing. *Anal Bioanal Chem.* **2006,** 384, 620-630.
5. Gillies, E.; Frechet, J. Dendrimers and dendritic polymers in drug delivery. *Drug Disc. Today.* **2005,** 10, 35-43.
6. Pinto Reis, C.; Neufeld, R. J.; Ribeiro, A. J.; Veiga, F. Nanoencapsulation II. Biomedical applications and current status of peptide and protein nanoparticulate delivery systems. *Nanomedicine.* **2006,** 2, 53-65.
7. Tomalia, D. A.; Regna, L. A.; Svenson, S. Dendrimers as multi-purpose nanodevices for oncology and diagnostic imaging. *Biochem Soc Trans.* **2007,** 35, 61-67.
8. Gabizon, A.; Shmeeda, H.; Barenholz, Y. Pharmacokinetics of Pegylated liposomal doxorubicin. *Clin Pharmacokinet.* **2003,** 42, 419-436.
9. Kratz, F.; Beyer, U.; Roth, T.; Tarasova, N.; Collery, P.; Lechenault, F.; Cazabat, A.; Schumacher, P.; Unger, C.; Falken, U. Transferrin conjugates of doxorubicin: Synthesis, characterization, cellular uptake and in vitro efficacy. *Journal of Pharmaceutical Sciences.* **1998,** 87, 338-346.
10. Chau, Y.; Dang, N. M.; Tan, F. E.; Langer, R. Investigation of targeting mechanism of new dextran-peptide-methotrexate conjugates using biodistribution study in matrix-metalloproteinase-overexpressing tumor xenograft model. *J Pharm Sci.* **2006,** 95, 542-551.
11. Chau, Y.; Padera, R. F.; Dang, N. M.; Langer, R. Antitumour efficacy of a novel polymer-peptide-drug conjugate in human tumou xenograft models. *Int. J. Cancer.* **2005,** 118, 1519-1526.
12. Lee, C.; Gillies, E.; Fox, M.; Guillaudeu, S.; Frechet, L.; Dy, E.; Szoka, F. A single dose of doxorubicin-functionalized bow-tie dendrimer cures mice bearing C-26 colon carcinomas. *Proc. Natl. Acad. Sci. U.S.A.* **2006,** 103, 16679-16654.
13. Wunder, A.; Stehle, G.; Schrenk, H. H.; Hartung, G.; Heene, D. L.; Mailer-Borst, W.; Sinn, H. Antitumour activity of methotrexate-albumin conjugates in rats bearing a walker-256 carcinoma. *Int. J. Cancer.* **1998,** 76, 884-890.
14. Gurdag, S.; Khandare, J.; Stapels, S.; Matherly, L. H.; Kannan, R. M. Activity of dendrimer-methotrexate conjugates on methotrexate-sensitive and -resistant cell lines. *Bioconjugate Chemistry.* **2006,** 17, 275-283.
15. Kono, K.; Liu, M.; Frechet, J. M. Design of dendritic macromolecules containing folate or methotrexate residues. *Bioconjugate Chemistry.* **1999,** 10, 1115-1121.
16. Kukowska-Latallo, J. F.; Candido, K. A.; Cao, Z.; Nigavekar, S. S.; Majoros, I. J.; Thomas, T. P.; Balogh, L. P.; Khan, M. K.; Baker, J. R. Nanoparticle targeting of anticancer drug improves therapeutic response in animal model of human epithelial cancer. *Cancer Res.* **2005,** 65, 5317-5324.

17. Gillies, E. R.; Dy, E.; Frechet, J. M. J.; Szoka, F. C., Jr. Biological Evaluation of Polyester Dendrimer: Poly(ethylene oxide) "Bow-Tie" Hybrids with Tunable Molecular Weight and Architecture. *Mol. Pharm.* **2005,** 2, (2), 129-138.
18. Lim, J.; Guo, Y.; Rostollan, C. L.; Stanfield, J.; Hsieh, J. T.; Sun, X.; Simanek, E. E. The role of the size and number of polyethylene glycol chains in the biodistribution and tumour localization of triazine dendrimers. *Molecular Pharmaceutics.* **2008,** 5, 540-547.
19. Malik, N.; Evagorou, E. G.; Duncan, R. Dendrimer-platinate: a novel approach to cancer chemotherapy. *Anti-Cancer Drugs.* **1999,** 10, (8), 767-776.
20. Okuda, T.; Kawakami, S.; Maeie, T.; Niidome, T.; Yamashita, F.; Hashida, M. Biodistribution characteristics of amino acid dendrimers and their PEGylated derivatives after intravenous administration. *Journal of Controlled Release.* **2006,** 114, 69-77.
21. Wu, G.; Barth, R.; Yang, W.; Kawabata, S.; Zhang, L.; Green-Church, K. Targeted delivery of methotrexate to epidermal growth factor receptor-positive brain tumors by means of cetuximab (IMC-C225) dendrimer bioconjugates. *Mol Cancer Ther.* **2006,** 5, 52-59.
22. Kaminskas, L. M.; Boyd, B. J.; Karellas, P.; Krippner, G. Y.; Lessene, R.; Kelly, B.; Porter, C. J. H. The impact of molecular weight and PEG chain length on the systemic pharmacokinetics of PEGylated poly-L-lysine dendrimers. *Mol Pharm.* **2008,** 5, 449-463.
23. Boyd, B. J.; Kaminskas, L. M.; Karellas, P.; Krippner, G.; Lessene, R.; Porter, C. J. H. Cationic Poly-L-Lysine Dendrimers: Pharmacokinetics, Biodistribution and Evidence for Metabolism and Bioresorption after Intravenous Administration in Rats. *Mol Pharm.* **2006,** 3, 614-627.
24. Francis, C. L.; Yang, Q.; Hart, N. K.; Widmer, F.; Manthey, M. K.; He-Williams, H. M. Total synthesis of methotrexate-TRIS-fatty acid conjugates. *Aust. J. Chem.* **2002,** 55, 635-645.
25. Kaminskas, L. M.; Zu, Z.; Barlow, N.; Krippner, G. Y.; Boyd, B. J.; Porter, C. J. H. Partly-PEGylated poly-L-lysine dendrimers have reduced plasma stability and circulation times compared with fully-PEGylated dendrimers. *J Pharm Sci.* **2009,** accepted 18/1/09.
26. Kaminskas, L.; Boyd, B. J.; Karellas, P.; Henderson, S. A.; Giannis, M. P.; Krippner, G.; Porter, C. J. Impact of surface derivatisation of poly-L-lysine dendrimers with anionic arylsulphonate or succinate groups on intravenous pharmacokinetics and disposition. *Mol Pharm.* **2007,** 4, 949-961.
27. Rennke, H. G.; Venkatachalam, M. A. Glomerular permeability of macromolecules. Effect of molecular configuration on the fractional clearance of uncharged dextran and neutral horseradish peroxidase in the rat. *J Clin Invest.* **1979,** 63, 713-717.
28. Malik, N.; Wiwattanapatapee, R.; Klopsch, R.; Lorenz, K.; Frey, H.; Weener, J. W.; Meijer, E. W.; Paulus, W.; Duncan, R. Dendrimers: Relationship between structure and biocompatibility in vitro, and preliminary studies on the biodistribution of I-125-labelled polyamidoamine dendrimers in vivo. *J. Control. Release.* **2000,** 65, 133-148.
29. Wang, S.; Lee, R. L.; Mathias, C. J.; Green, M. A.; Low, P. S. Synthesis, purification, and tumor cell uptake of 67Ga-desferoxamine-folate, a potential radiopharmaceutical for tumor imaging. *Bioconjugate Chemistry.* **1996,** 7, 56-62.
30. Rosowsky, A.; Forsch, R.; Uren, J.; Wick, M. Methotrexate analogues, 14. Synthesis of new gamma-substituted derivatives as dihydrofolate reductase inhibitors

and potential anticancer agents. *Journal of Medicinal Chemistry.* **1981,** 24, 1450-1455.

31. Han, Y. H.; Kato, Y.; Sugiyama, Y. Binding and transport of methotrexate and its derivative MX-68, across the brush-border membrane in rat kidney. *Biopharmaceutics and drug disposition.* **1999,** 20, 361-367.